

# Cyclostationarity Detection of DVB-T Signal: Testbed and Measurement

Matthieu Gautier<sup>1</sup>, Marc Laugeois<sup>1</sup> and Philippe Hostiou<sup>2</sup>

<sup>1</sup>CEA, LETI, Minatec, Grenoble, France,

<sup>2</sup>TeamCast, Centre Espace Performance, F35769 Saint-Grégoire, France,  
matthieu.gautier1@cea.fr, marc.laugeois@cea.fr, philippe.hostiou@teamcast.com

**Abstract**—In this paper, realistic performance of Digital Video Broadcasting - Terrestrial (DVB-T) spectrum sensing are investigated for cognitive radio applications. To this end, an implementation of a cyclostationarity detector is proposed as an efficient means for signal detection under low Signal to Noise Ratio (SNR) conditions. This paper focuses on the design of a hardware testbed that performs the cyclostationarity detection, and introduces a measurement campaign that has been performed in order to have a realistic validation of the proposed solution. Measurement results show that SNR down to -6 dB could be detected by our hardware demonstrator.

**Keywords**—TV White Spaces, Cyclostationarity detection, FPGA, Measurement.

## I. INTRODUCTION

The performance of sensing algorithms is fundamental in establishing the opportunistic communication of a cognitive radio (CR) system [1]. Many scenarios have been investigated in the context of CR network. The most likely to occur in the short term is the unlicensed usage of TV bands often referred to as the TV White Space (TVWS) scenario. This scenario was made possible by the FCC in the US in 2008, with some restrictions which include high-sensitivity requirements for primary user detection [2]. In the context of this scenario, standardization has been very active, especially under the IEEE802.22 banner [3].

In Europe, the TV bands primary user is the DVB-T transmitters and cyclostationarity detector has been proposed as the most promising technique for DVB-T signal sensing. By using cyclostationary features induced by the Cyclic Prefix (CP), it allows OFDM (Orthogonal Frequency Division Multiplexing) based signals detection at low SNR.

If the theoretical aspect of this detector has been thoroughly addressed in literature [4][5][6], solutions need to be proposed for its hardware implementation in order to achieve a good architecture-performance tradeoff. Indeed, in an operational system, the sensing block has to be implemented on a real hardware platform. Then, all theoretical functions have to be expressed as logical blocks and an explicit dimensioning of all links between blocks and data format must be carefully performed. In [7], an efficient implementation of a cyclostationarity detector was proposed by our team. The *a priori* knowledge of the DVB-T signal nature helps avoid the implementation of a large FFT operator as used in the state of the art architectures [8][9].

This paper focuses on the design of a testbed that performs the hardware architecture introduced in [7] that performs the detection of DVB-T signals for the TVWS scenario. Some spectrum sensing testbeds have already been developed: most of them concern the energy detection [10][11] or collaborative sensing [10][12] and those that deal with cyclostationarity detection are high level demonstration [13] or dedicated to other bands (802.11n [14] and 802.11g [15]), not dedicated to the TVWS scenario.

The other objective of this paper is to achieve realistic performance of the cyclostationarity detector using the proposed testbed. To this end, a measurement campaign has been performed with the platform and results from these measurements are given in this paper.

This paper consists of 5 parts. Following this introduction, Section II introduces the cyclostationarity detector and its hardware implementation dedicated to DVB-T signals. In Section III, the platform used for the demonstration is described. Section IV details the experimental validation of the detector by giving some measurement results. Finally, conclusions are drawn and outlook is provided.

## II. CYCLOSTATIONARITY DETECTOR FOR DVB-T SIGNALS

This section derives the theoretical equation used by cyclostationarity detector and introduced the hardware architecture (presented in [7]) suitable to DVB-T signals.

### A. Cyclostationarity based OFDM detector

For the DVB-T signal sensing, the proposed technique is based on the *a priori* knowledge of the OFDM modulation based DVB-T physical layer. The algorithm, described in [6] aims at detecting the cyclostationarity of the DVB-T signal through the analysis of the Fourier decomposition of its second order momentum. It exploits the structure of the OFDM symbols which contains the same pattern at its beginning and end; the so called cyclic prefix. By computing the autocorrelation of the incoming signal with a lag corresponding to the symbol duration, the cyclic prefix is emphasized while the rest of the correlation tends to zero. This is due to the fact that the data portion of the OFDM symbols is uncorrelated over consecutive symbols. Thus, the mathematical expectation of the correlation signal is time periodic, also referred to as the cyclostationary nature of the OFDM signal  $s[n]$ .

Let us now consider the autocorrelation of this signal:

$$R_s(u, m) = E \{s[u + m]s^*[u]\}. \quad (1)$$

Under the condition that all subcarriers are used, the autocorrelation of an OFDM signal is written as [6]:

$$R_s(u, m) = R_s(u, 0) + R_s(u, N)\delta(m - N) \dots \\ \dots + R_s(u, -N)\delta(m + N), \quad (2)$$

with  $N$  being the number of subcarriers and  $\delta$  being the Dirac function.

The first term of (2) is the power of the received signal. Energy detectors, derived only from this term, provide poor performance at low SNR. To increase the performance of the detector at low SNR, we focus on the last two terms of (2) to build a cost function. The terms  $R_s(u, N)$  and  $R_s(u, -N)$  correspond to the correlation induced by the cycle prefix. It can be shown [16] that  $R_s(u, N)$  is a periodic function of  $u$  which characterizes the signal  $s$ .  $R_s(u, N)$  has a period  $\alpha_0^{-1} = N + D$  with  $D$  being the length of the cyclic prefix. As this function depends on  $u$  in a periodic way, the signal is not a stationary but a cyclostationary signal. Its autocorrelation function can be written as a Fourier series:

$$R_s(u, N) = R_s^0 + \sum_{k=-\frac{N+D}{2}, k \neq 0}^{\frac{N+D}{2}-1} R_s^{k\alpha_0}(N)e^{2i\pi k\alpha_0 u}. \quad (3)$$

In (3),  $R_s^{k\alpha_0}$  is the cycle correlation coefficient at cycle frequency  $k\alpha_0$  and at time lag  $N$ . This term can be estimated as follows:

$$R_s^{k\alpha_0}(N) = \frac{1}{U} \sum_{u=0}^{u-1} s(u + N)s^*(u)e^{-2i\pi k\alpha_0 u}, \quad (4)$$

where  $U$  is the observation time.

The basic idea behind the cyclostationarity detector is to analyze this Fourier decomposition and assess the presence of the signal by setting a cost function related to one or more of these cyclic frequencies. This cost function is compared to some reference value. This technique was introduced in a more general context in the early 90s by Gardner [17][16]. Recent papers have applied this approach to the opportunistic radio context [4][5][6]. They mainly differ in the way the harmonics are considered. In our study, the proposed cost function exploits both the fundamental and several harmonics as expressed in (5):

$$J_s(K_s) = \frac{1}{2K_s + 1} \sum_{k=-K_s}^{K_s} |R_s^{k\alpha_0}(N)|^2, \quad (5)$$

where  $K_s$  is the number of harmonics that are considered.

It can be observed that the cost function is only built upon  $R_s(u, N)$ , while  $R_s(u, -N)$  is omitted. Indeed, it is quite easy to prove that  $|R_s^{k\alpha_0}(N)|^2 = |R_s^{k\alpha_0}(-N)|^2$  [6].

Introduced in [7], the hardware integration of this algorithm is presented in the following chapter.

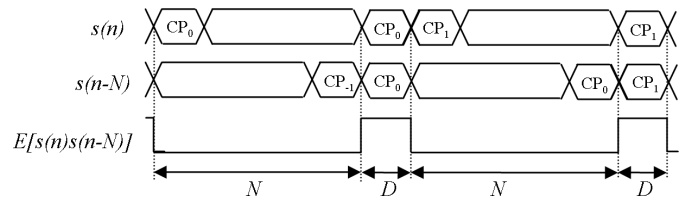


Figure 1. Ideal autocorrelation signal of an OFDM symbol burst.

### B. Hardware architecture for DVB-T detector

The DVB-T standard defines three FFT sizes:  $N=2048$ , 4096 or 8192 for a channel bandwidth  $B_s$  of 8MHz. The cyclic prefix over FFT size ratio  $D/N$  can also vary: 1/32, 1/16, 1/8, 1/4. Considering all the configurations leads to very highly complex hardware architecture. However, in practice, deployment considers a smaller set of parameters depending on the country. For instance, in France, the set of parameters used is  $N=8192$  and  $D/N=1/32$ , only this set will be used to design our architecture.

A key characteristic that will be exploited in the architecture design stems from the broadcast nature of the DVB-T signal. This means that detector sensitivity can be increased significantly by very long integration time. This is a relevant feature since sensitivity requirements for primary user detection are very challenging (typically SNR=-10dB [18]). It also changes the way that the reference signal is used to define the decision variable. When undertaking this calibration phase, the secondary system needs to consider a reference noise value which is independent of the signal presence.

When considering long (ideally infinite) integration time, the autocorrelation function defined in previous section tends to a rectangular signal as depicted in Fig. 1, the cyclic ratio being  $\frac{D}{N+D}$ . In this case, the Fourier coefficient is written as:

$$R_s^{k\alpha_0}(N) = \frac{A}{2\pi k} \left\{ \sin\left(\frac{2\pi k D}{N+D}\right) + j \left(1 - \cos\left(\frac{2\pi k D}{N+D}\right)\right) \right\}, \quad (6)$$

Each coefficient power is given by:

$$|R_s^{k\alpha_0}(N)|^2 = \begin{cases} \left(\frac{AD}{N+D}\right)^2, & k = 0, \\ 2 \left(\frac{A}{2\pi k}\right)^2 \left(1 - \cos\left(\frac{2\pi k D}{N+D}\right)\right), & k \neq 0. \end{cases} \quad (7)$$

#### Decision variable computation:

First, a reference noise level has to be computed from the observation in order to be compared with the signal cost function  $J_s(K_s)$ . It is obvious from equation (7) that  $R_s^{k\alpha_0}(N) = 0$  when  $k = l\left(\frac{N}{D} + 1\right)$ ,  $l = \{1, 2, \dots + \infty\}$ . The Fourier harmonics  $l\left(\frac{N}{D} + 1\right)$  are not impacted by the presence of the signal and can thus be used for calibration purpose to define the reference noise level. Similarly to (5), a cost function  $J_n$  could be defined in order to compute the noise level:

$$J_n(K_n) = \frac{1}{2K_n} \sum_{l=-K_n, l \neq 0}^{K_n} \left| R_s^{l\left(\frac{N}{D} + 1\right)\alpha_0}(N) \right|^2, \quad (8)$$

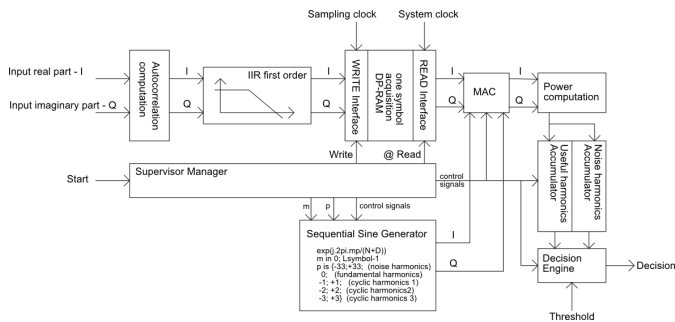


Figure 2. Cyclostationarity detector for DVB-T signals.

with  $K_n$  being the number of harmonics that are considered. For example, considering the French set of parameters ( $D/N=1/32$ ) and considering the first 4 signal harmonics  $-3;+3$  and one noise harmonic (i.e.,  $K_s=3$  and  $K_n=1$ ), the decision variable  $V$  can be expressed as follows:

$$V = \frac{J_s(K_s)}{J_n(K_n)} = \frac{2}{7} \frac{\sum_{k=-3}^3 |R_s^{k\alpha_0}(N)|^2}{|R_s^{-33\alpha_0}(N)|^2 + |R_s^{33\alpha_0}(N)|^2}. \quad (9)$$

**Hardware architecture:**

Introduced in [7], the proposed cyclostationarity detector hardware architecture is shown in Fig. 2 for the parameters  $K_s = 3$  and  $K_n = 1$ .

First, the autocorrelation is computed on the I/Q complex samples. The IIR (Infinite Impulse Response) integrator then averages over a number of symbols tuned by setting the integration time parameter to achieve the required sensitivity. The supervisor, a Finite State Machine (FSM), then triggers the writing into a buffer that stores 8192 filter output samples (equivalent to the length of an OFDM symbol). Then, using a faster clock, the Fourier harmonics are computed sequentially. The sine generator computes sequentially the required sine function of the Fourier taps of interest. The Multiply ACCumulate (MAC) function enables the Fourier coefficient to be obtained for these taps. The sequence is as follows. First the reference harmonics  $-33; +33$  are generated to compute the noise reference power. Then the harmonics of interest for the DVB-T signal  $0;-1;+1;-2;+2;-3;+3$  are calculated. The power of each harmonic is summed up to obtain the cyclostationarity estimator value. Finally the decision engine gives the final result by comparing the estimated value to the decision value according to (9), which provides a hard decision output of the detector.

This technique holds theoretically for infinite integration time to guarantee the rectangular shape of the autocorrelation estimator. Whenever a finite integration is performed, detection performance is improved by increasing the integration ability

	Complexity			Latency
	Slices	RAM blocks of 18kbits	Mult	
Detector	1600	122	23	Depends on n
Total	25280	232	128	

TABLE I. COMPLEXITY EVALUATION OF THE DVB-T DETECTOR.



Figure 3. Platform overview.

of the filter. The integration ability of the filter depends on the length of the filter denoted  $n$ .

The complexity of such a detector hardware implementation is determined on a Xilinx Virtex 4 target technology using the ISE XST synthesis tool. Results are provided in Table I. The complexity is compared with the total resource available in the FPGA. Table I shows that 6% of the slices, 52% of the RAM blocks and 17% of the multipliers have been used to perform the detection. If the final implementation will integrate this detector and a PHY layer for the opportunistic communication, this complexity seems quite high (especially the memory blocks) and a new version of Xilinx FPGA should be used for the final implementation.

**III. TESTBEDS DESCRIPTION AND SPECIFICATIONS**

*A. Overview of the demonstrator*

Fig. 3 shows the testbed used to validate the detection of DVB-T signal. The testbed consists of two parts:

- The modulator is a standard TeamCast DVB-T products [19]. A video stream is pulse shaped and transposed in the TV channel according to the DVB-T standard. It emulates a base station broadcast of the DVB-T network.
- The receiver performs two functions: the "sensing block" and the "DVB-T demodulator". It then provides a video stream and the decision variable provided by the detector.

A PC controls and supervises the testbeds using RS232 links. Three software Human-Machine interfaces have been developed, one to control the setting of the DVB-T modulator, one for the DVB-T demodulator and one that controls the detector characteristics and supervises the measurements.

A measurement consists in scanning a 8MHz UHF channel and then in detecting if this channel is vacant. The detection is based on the decision variable as defined by (9).

*B. Hardware specification of the receiver*

Fig. 4 provides an overview of the architecture of the receiver used to test the proposed architecture. The receiver is composed of two parts: a RF board that performs the translation of the RF UHF signal to IQ baseband signal and a digital board that executes the baseband algorithms.

The RF board is composed of an analog part and a digital part. The analog Downconverter block allows the transposition of the UHF band (470 - 860MHz) to an Intermediate Frequency (IF) of 240MHz. An Analog to Digital Converter (ADC) then converts the signal into samples. The sampling frequency is 73.4 Mhz corresponding to 8 times the symbol

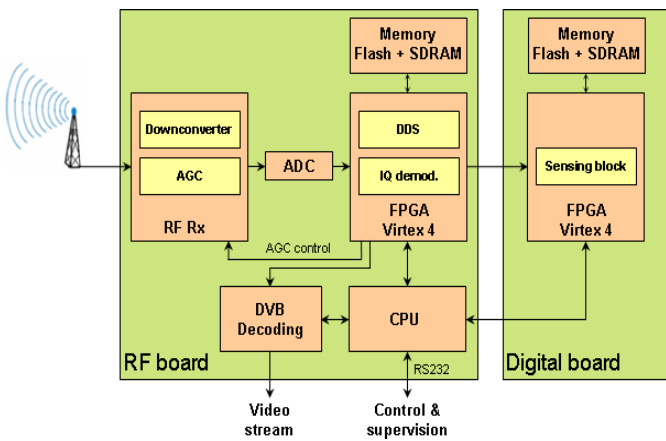


Figure 4. Receiver architecture.

frequency  $F_s$ . To ensure a constant level at the input of the ADC, two automatic gain control (AGC) loops are implemented, one at RF and one at IF.

The digital IF signal is then processed by an FPGA that performs the baseband transposition. The different elements are: a bandpass filter that attenuates the adjacent channels, an I/Q demodulation, a Direct Digital Synthesizer (DDS) that performs the baseband translation and finally decimators to switch from  $8F_s$  to  $F_s$ .

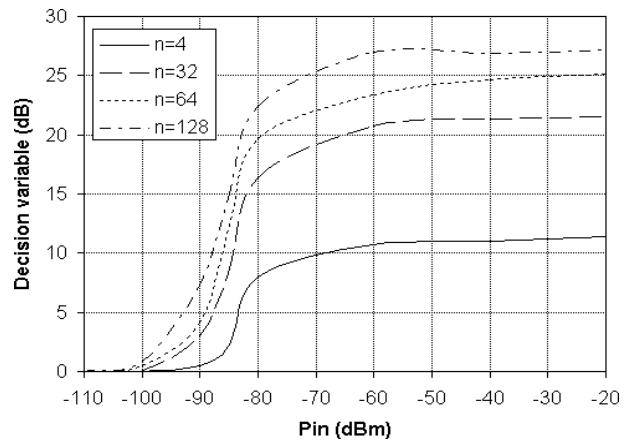
The IF and RF AGC guarantee the level of the digital signal into the range between -75 dBm and -35 dBm. The power is computed using the outputs of the ADC. The gain of the AGC is linear within this range, thus ensuring no distortion of the input signal. The RF board also contains a specific chip that performs the DVB-T decoding.

This I/Q stream is then transmitted to the Digital board via a high-speed serial link. The I/Q samples are received at the frequency  $F_s$  of 64/7 MHz. The digital board is composed of an FPGA Xilinx Virtex-4 FX60 and memories (both SDRAM and flash). The hardware architecture of the detector detailed in Section II is implemented on this board.

An important remark is that the IF AGC has not been integrated in the platform reducing the range of the input signal. Under this condition, the thermal noise of the receiver  $P_{Th}$  has been measured at -80 dBm.

#### IV. EXPERIMENTAL MEASUREMENTS

In this section, realistic performance results of the proposed detector are given from a measurement campaign. In this campaign, the channel is considered to be an AWGN (Additive White Gaussian Noise) one as Line of Sight conditions are performed. In our scenario, the primary system is the French DVB-T (i.e., FFT size of 8192 and a cyclic prefix of 1/32). First, the false alarm are induced by the thermal noise and, then, by a secondary system that already communicates in the channel.

Figure 5. Mean of decision variable versus  $P_{in}$  for different filter length  $n$ .

#### A. Decision variable distribution

First, we observed the distribution of the decision variable  $V$  according to (9) as a function of the receiver input power  $P_{in}$ . In practice, the power of noise harmonic comes from two sources: the thermal noise  $P_{Th}$ , which is constant, and the autocorrelation noise which is proportional to the input power  $P_A = k_A P_{in}$ . The power of useful harmonics is also proportional to the input power. Assuming that, in the useful harmonics, the power of the thermal noise is negligible relative to the power of the signal, the decision variable  $V$  can be written:

$$V = \frac{kP_{in}}{P_{Th} + k_A P_{in}} = \frac{k}{\frac{1}{SNR} + k_A}, \quad (10)$$

with  $k$  and  $k_A$  constant,  $SNR = P_{in}/P_{Th}$  and  $kP_{in} \gg P_{Th}$ .

Fig. 5 shows the mean of decision variable  $V$  versus  $P_{in}$  for different filter length  $n=4, 32, 64$  and 128.

According to the curves of Fig. 5, three ranges of receiver input power can be distinguished:

- Range 1: When the input received power is lower than -100 dBm, (10) is no longer valid, and the noise becomes dominant compared to the signal. The harmonics are only noise harmonics and  $V=0$  dB.
- Range 2:  $P_{in}$  for between -100 dBm and -80 dBm, the curve is approximately linear, and  $V$  is proportional to  $P_{in}$ .
- Range 3: For powers higher than -70 dBm,  $V$  is constant and only depends on  $n$ .

Finally, we note the influence of the filter length  $n$ . The larger  $n$  is, the higher the decision variable is. For high input powers (range 3),  $V$  is 11 dB for  $n=4$  and 27 dB for  $n=128$ .

#### B. Detection probability

The detection probability  $p_D$  is the probability that the system detects the DVB-T signal when it is present in the channel. These probabilities are obtained (leading to a false alarm probability of 10%) when the detector is matched with the transmitter (i.e., FFT size of 8192 and a cyclic prefix of 1/32). Measurements are performed for different received power levels of the primary signal ( $-90 \text{ dBm} < P_{in} < -70 \text{ dBm}$ ).

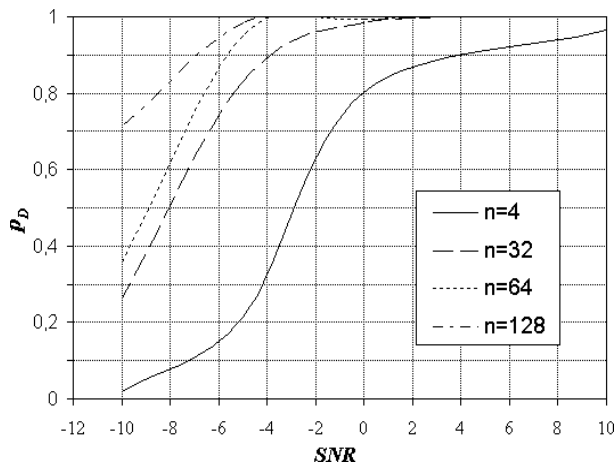


Figure 6. Detection probability versus  $SNR$  for different filter length  $n$ .

Fig. 6 shows the performance of the algorithm for different filter length  $n = 4, 32, 64$  and  $128$ .

Thus, for the detection of a DVB-T signal (8k, 1/32) and a target of 95% of successful detection, the measurement results show that the detection of  $SNR$  down to 10 dB could be achieved with a filter length  $n=4$ ,  $SNR$  down to -2 dB with  $n=32$ ,  $SNR$  down to -5 dB with  $n=32$  and  $SNR$  down to -6 dB with  $n=128$ .

### C. False alarm: Another DVB-T signals

So far, the false alarms correspond to the case where the detector detects a signal while no signal is present at the receiver input. In this part, we analyse another kind of false alarms: when a secondary transmitter uses the same channel with a DVB-T signal having different characteristics than the primary transmitter DVB-T.

The detector is set on an FFT of 8192, a cyclic prefix of 1/32 and a filter size  $n=64$ . To test the influence of the size of the cyclic prefix, the false alarm probability is computed for a secondary transmitter using cyclic prefix of 1/16, 1/8 and 1/4 (with a given FFT size of 8192). To test the influence of the size of the FFT, the false alarm probability is computed for a secondary transmitter using FFT sizes of 4096 and 2048 (with a given cyclic prefix of 1/32).

The measurements are performed under high SNR conditions (input power  $P_{in}$  of -40 dBm). The detection probability  $p_D$  is plotted versus the false alarm probability  $p_{FA}$  for different sizes of cyclic prefix (Fig. 7) and for different sizes of FFT (Fig. 8).

The measurement results show that the size of the cyclic prefix has more influence on the number of false alarm than the length of the FFT. Thus, when the secondary transmitter uses an FFT of 8192 and a cyclic prefix different from the one of the detector, the detection probability is decreasing, the detection being impossible for  $CP=1/16$ . However, if the secondary transmitter uses an FFT size different than the one used by the detector, the number of false alarm is low and the detection is feasible.

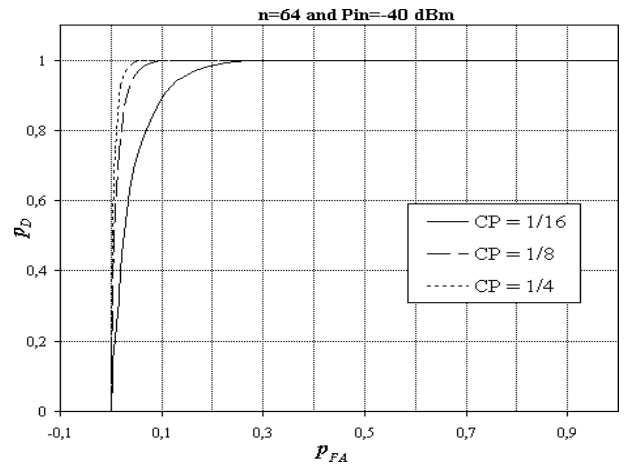


Figure 7. Detection probability versus false alarm probability for different sizes of cyclic prefix.

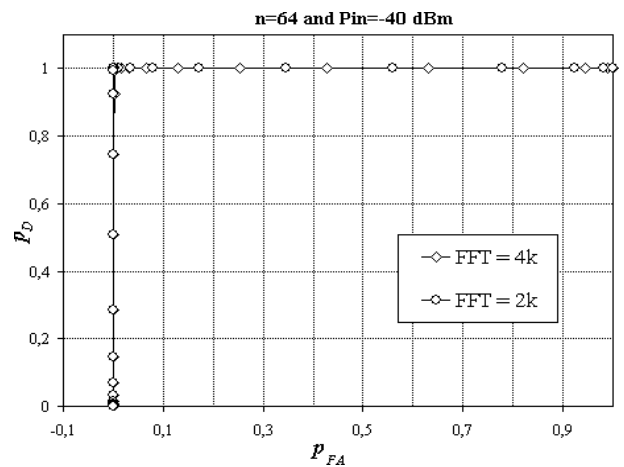


Figure 8. Detection probability versus false alarm probability for different sizes of FFT.

## V. CONCLUSIONS AND FUTURE WORKS

Scenarios have a strong influence on architecture and its performance tradeoffs. In the secondary spectrum usage of licensed TV bands, interference is not allowed, and much attention must be paid to sensitivity. In this paper, DVB-T signal sensing has been addressed using the cyclostationarity detector. The motivation of this study is to achieve realistic performance of this detector for the TVWS scenario. This paper focuses on the design of a hardware testbed that performs the cyclostationarity detection and introduces a measurement campaign.

The receiver could not reach very low sensitivity because only one AGC has been implemented. However, this limitation is not prohibitive in the use of the algorithm. We have shown that, with a thermal noise of -80 dBm, the architecture could achieve the detection of  $SNR$  down to -6 dB.

The influence of the filter length has been highlighted with a 16 dB sensitivity gain between  $n=4$  and  $n=128$ . Finally, the false alarm and detection performance will help the setting of the detection threshold according to the desired strategy of detection.

Future work is to update the RF board of the receiver with the integration of the IF AGC and to perform measurements with realistic broadcast channel conditions [20] with both multipaths and frequency dispersive characteristics.

#### ACKNOWLEDGMENT

The research leading to these results was derived from the French national project ANR-INFOP.

#### REFERENCES

- [1] J. Mitola III and G. Q. Maguire Jr, "Cognitive radio: making software radios more personal," *IEEE Personal Communications*, vol. 6, no. 4, pp. 13–18, 1999.
- [2] Official announcement of FCC, "FCC adopts rules for unlicensed use of television white spaces," available from <http://www.fcc.gov>, 15.03.2011, November 2008.
- [3] IEEE 802.22, "Wireless Regional Area Networks ("WRANs")," available from <http://www.ieee802.org/22/>, 15.03.2011.
- [4] M. Ghozzi, M. Dohler, F. Marx, and J. Palicot, "Cognitive Radio: Methods for Detection of Free Bands," *Elsevier Science Journal, Special Issue on Cognitive Radio*, vol. 7, Sept 2006.
- [5] J. Lunden, V. Koivunen, A. Huttunen, and H. Vincent Poor, "Spectrum Sensing in Cognitive Radios Based on Multiple Cyclic Frequencies," <http://arxiv.org/abs/0707.0909>, 15.03.2011, July 2007.
- [6] P. Jallon, "An algorithm for detection of DVB-T signals based on their second order statistics," *EURASIP journal on wireless communications and network*, 2008.
- [7] Dominique Noguét, Lionel Biard, and Marc Laugeois, "Cyclostationarity Detectors for Cognitive Radio: Architectural Tradeoffs," *EURASIP Journal on Wireless Communications and Networking*, 2020.
- [8] V. Turunen, M. Kosunen, A. Huttunen, S. Kallioinen, P. Ikonen, A. Pärssinen, and J. Rynänen, "Implementation of cyclostationary feature detector for cognitive radios," *IEEE International Conference on Cognitive Radio Oriented Wireless Networks and Communications (CROWNCOM09)*, June 2009.
- [9] Y. Tachwali, M. Chmeiseh, F. Basma, and H. H. Refai, "A frequency agile implementation for IEEE 802.22 using software defined radio platform," *IEEE Globecom 2008*, December 2008.
- [10] D. Cabric, A. Tkachenko, and R. W. Brodersen, "Experimental study of spectrum sensing based on energy detection and network cooperation," *ACM 1st Int. Workshop on Technology and Policy for Accessing Spectrum (TAPAS06)*, August 2006.
- [11] J.Y. Xu and F. Alam, "Adaptive energy detection for cognitive radio: An experimental study," *IEEE International Conference on Computers and Information Technology (ICCIT09)*, December 2009.
- [12] S.M. Mishra, D. Cabric, C. Chang, D. Willkomm, B. Van Schewick, S. Wolisz, and B.W. Brodersen, "A Real Time Cognitive Radio Testbed for Physical and Link Layer Experiments," *IEEE New Frontiers in Dynamic Spectrum Access Networks (DySPAN05)*, Nov. 2005.
- [13] M. Ghozzi, B. Zayen, and A. Hayar, "Experimental Study of Spectrum Sensing Based on Distribution Analysis," *18th ICT-MobileSummit Conference*, June 2000.
- [14] S. Kandeepan, G. Baldini, and R. Piesiewicz, "Experimentally detecting IEEE 802.11n Wi-Fi based on cyclostationarity features for ultra-wide band cognitive radios," *IEEE International Symposium on Personal, Indoor and Mobile Radio Communications (PIMRC09)*, Sept. 2009.
- [15] L. Biard, D. Noguét, T. Gernandt, P. Marques, and A. Gameiro, "A hardware demonstrator of a cognitive Radio system using temporal opportunities," *IEEE International Conference on Cognitive Radio Oriented Wireless Networks and Communications (CROWNCOM09)*, June 2009.
- [16] W. A. Gardner and M. Spooner, "Signal Interception: Performance Advantages of Cyclic-Feature Detectors," *IEEE Transactions on Communications*, vol. 40, no. 1, Jan 1992.
- [17] W. A. Gardner and G. Zivanovic, "Degrees of cyclostationary and their application to signal detection and estimation," *IEEE Signal Processing*, vol. 22, no. 3, March 1991.
- [18] S. J. Shellhammer, "Spectrum sensing in IEEE 802.22," *IAPR Workshop on Cognitive Information Processing*, June 2008.
- [19] TeamCast, "Description of DVB-T modulator," available from <http://www.teamcast.com/en/maj-e/c2a2i19508/>, 15.03.2011.
- [20] TeamCast, "Description of RF Channel Simulator," available from <http://www.teamcast.com/en/maj-e/c1a2i19493/>, 15.03.2011.